

# Physics-informed deep learning for incompressible laminar flows

Chengping Rao<sup>a</sup>, Hao Sun<sup>b,c</sup>, Yang Liu<sup>a,\*</sup>

<sup>a</sup>Department of Mechanical and Industrial Engineering, Northeastern University, Boston, MA 02115, USA

<sup>b</sup>Department of Civil and Environmental Engineering, Northeastern University, Boston, MA 02115, USA

<sup>c</sup>Department of Civil and Environmental Engineering, MIT, Cambridge, MA 02139, USA

---

## Abstract

Physics-informed deep learning (PIDL) has drawn tremendous interest in recent years to solve computational physics problems. The basic concept of PIDL is to embed available physical laws to constrain/inform neural networks, with the need of less rich data for training a reliable model. This can be achieved by incorporating the residual of the partial differential equations and the initial/boundary conditions into the loss function. Through minimizing the loss function, the neural network would be able to approximate the solution to the physical field of interest. In this paper, we propose a mixed-variable scheme of physics-informed neural network (PINN) for fluid dynamics and apply it to simulate steady and transient laminar flows at low Reynolds numbers. The predicted velocity and pressure fields by the proposed PINN approach are compared with the reference numerical solutions. Simulation results demonstrate great potential of the proposed PINN for fluid flow simulation with a high accuracy.

*Keywords:* Physics-informed neural networks (PINN), deep learning, fluid dynamics, incompressible laminar flow

---

## 1. Introduction

Deep learning (DL) has attracted tremendous attentions in recent years in the field of computational mechanics due to its powerful capability in nonlinear modeling of complex spatiotemporal systems. According to a technical report [1] by U.S. Department of Energy in 2018, a DL-based approach should be featured with the domain-aware, interpretable and robust to be a general approach for solving the science and engineering problems. Recent studies of leveraging DL to model physical system include, just to name a few, [2–6]. These applications can be categorized into two types based on how the DL model is constructed: in either data-driven or physics-informed manner. In a data-driven framework, the DL model is constructed as a black-box to learn a surrogate mapping from the formatted input  $\mathbf{x} \in \mathbb{R}^m$  to the output  $\mathbf{y} \in \mathbb{R}^n$ . The exceptional approximation ability of deep neural network (DNN) makes possible to learn the mapping even when the dimensionality  $m$  and  $n$  are very high. The training dataset  $\{\mathbf{x}, \mathbf{y}\}$ , typically very rich, can be obtained by conducting

high-fidelity simulations using exact solvers (e.g., see [3, 4, 7]). Nevertheless, obtaining a rich and sufficient dataset from simulations for training a reliable DL model is computationally expensive and requires careful case design. To address this fundamental challenge, physics-informed DL explicitly embed the physical laws (e.g., the governing partial differential equations (PDEs), initial/boundary conditions, etc.) into the DNN which provide rigorous constraint to the network trainable parameters within a feasible solution space. The objective of exploiting physical laws in DNN is assumed to (1) reduce the large dependency of the model on available dataset in terms of both quality and quantity, and (2) improve the robustness and interpretability of the DL model. In this regard, DNN essentially has the capacity of approximating the latent solutions for PDEs [8, 9], with distinct benefits summarized as follows: (1) the superior interpolation ability of DNN, (2) the approximated solution has a close form with its infinite derivative continuous, and (3) state-of-the-art hardware advances make the numerical implementation and parallelization extremely convenient.

More recently, Raissi *et al.* [5, 6] introduced a general framework of physics-informed neural network (PINN) and demonstrated its capacity in modeling complex physical systems such as solving/identifying

---

\*Corresponding author. Tel: +1 617-373-8560

Email addresses: [h.sun@northeastern.edu](mailto:h.sun@northeastern.edu) (Hao Sun),  
[yang1.liu@northeastern.edu](mailto:yang1.liu@northeastern.edu) (Yang Liu)

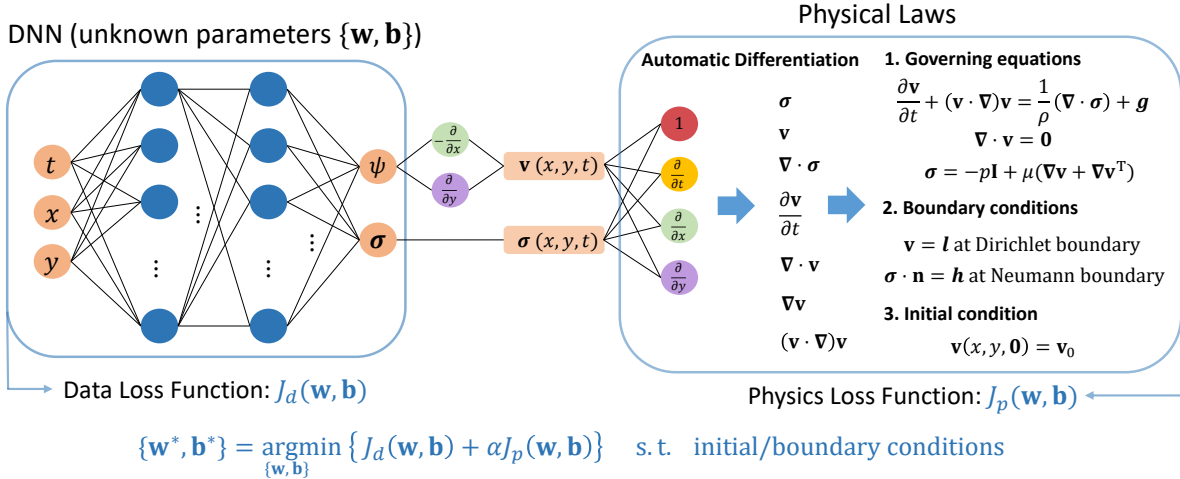


Figure 1: Architecture of the physics-informed neural network for fluid dynamics. Note that  $\alpha$  is a user-defined weighting coefficient.  $\mathbf{w}$  and  $\mathbf{b}$  are weights and biases for the DNN. The constraint of initial and boundary conditions can be converted as residuals adding to the loss function based on Lagrangian multipliers. The data loss  $J_d$  is present only when data is available.

PDEs. A huge difference from some of the previous studies is that, in addition to the physical laws, the PINN can also exploit the available measurement data, making it possible to discover the systems whose physics are not fully understood. In particular, seminal contributions of using PINN to model fluid flows have been made recently. For example, Kissas *et al.* [10] employed PINN to predict the arterial blood pressure based on the MRI data and the conservation laws. Sun *et al.* [11] proposed a PINN approach for surrogate modeling of fluid flows without any simulation data. Zhu *et al.* [12] proposed a physics-constrained convolutional encoder-decoder network and a generative model for modeling of stochastic fluid flows.

The main contribution of this paper is to formulate a mixed-variable PINN scheme for simulation of viscous incompressible laminar flows without any measurement data. The remaining this paper is organized as follows. In Section 2, we will introduce the methodology of the mixed-variable PINN and the mathematical formulation for fluid dynamics. Subsequently in Section 3, the steady and transient laminar flows passing a circular cylinder will be modeled using the proposed PINN scheme without any simulation data. The Section 4 summarizes the conclusions.

## 2. Methodology

Let us consider the incompressible Newtonian flow governed by the following NavierStokes equations:

$$\nabla \cdot \mathbf{v} = 0 \quad (1)$$

$$\frac{\partial \mathbf{v}}{\partial t} + (\mathbf{v} \cdot \nabla) \mathbf{v} = -\frac{1}{\rho} \nabla p + \frac{\mu}{\rho} \nabla^2 \mathbf{v} + \mathbf{g} \quad (2)$$

where  $\nabla$  is the Nabla operator,  $\mathbf{v} = (u, v)$  is the velocity vector,  $p$  is the pressure,  $\mu$  is the viscosity of the fluid,  $\rho$  is the density of fluid and  $\mathbf{g}$  is the gravitational acceleration. When leveraging PINN to solve the aforementioned PDEs, minimizing a complex residual loss resulted from Eq. (2) is intractable due to its complex form with multiple latent variables (e.g.,  $\mathbf{v}$  and  $p$ ) and high-order derivatives (e.g.,  $\nabla^2$ ). In order to design an easily trainable PINN, we convert the NavierStokes equation in Eq. (2) to the following continuum and constitutive formulations:

$$\frac{\partial \mathbf{v}}{\partial t} + (\mathbf{v} \cdot \nabla) \mathbf{v} = \frac{1}{\rho} \nabla \cdot \boldsymbol{\sigma} + \mathbf{g} \quad (3)$$

$$\boldsymbol{\sigma} = -p\mathbf{I} + \mu(\nabla \mathbf{v} + \nabla \mathbf{v}^T) \quad (4)$$

where  $\boldsymbol{\sigma}$  is the Cauchy stress tensor and  $p = \operatorname{tr}(\boldsymbol{\sigma})$ . The benefits of using the continuum-mechanics-based formulation are two-fold: (1) reducing the order of derivatives when a mixed-variable scheme in PINN is used, and (2) improved trainability of DNN as found in numerical implementations.

We propose a mixed-variable PINN scheme to solve the aforementioned PDEs (see Eqs. (1), (3) and (4)) that govern the laminar flow dynamics. The salient feature of PINN is that the physical fields are approximated globally by a DNN. In particular, the DNN maps the spatiotemporal variables  $\{t, \mathbf{x}\}^T$  to the mixed-variable solution  $\{\psi, \boldsymbol{\sigma}\}^T$ , where the stream function  $\psi$  is employed rather than the velocity  $\mathbf{v}$  to ensure the

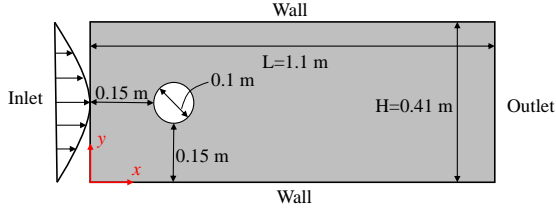


Figure 2: Diagram of the computation model.

divergence free condition of the flow. In this way, the continuity equation will be satisfied automatically. For a two-dimensional problem, the velocity components can be computed by  $[u, v, 0] = \nabla \times [0, 0, \psi]$ . Note that  $\mathbf{v} = [u, v]$  is taken as the latent variable. The technique called automatic differentiation makes possible to obtain the partial derivatives of the DNN output with regard to time and space (e.g.,  $t$ ,  $x$  and  $y$ ). The loss function for the training of the DNN is composed of the terms corresponding to the measurement data mean squares error  $J_d$ , the governing equation residual  $J_p$ , as well as the initial and boundary conditions  $J_{I/BC}$ . Noteworthy, having the measurement data makes the fluid flow modeling data-driven, which is however not a prerequisite. The architecture of the proposed PINN for fluid dynamics simulation is presented in Fig. 1. In this paper, no measurement data from simulations or physical experiments is used for training the PINN.

### 3. Results

In this section, we test the performance of the proposed PINN for modeling flows passing a circular cylinder. Both the steady and transient cases are considered to verify the proposed approach. The schematic diagram of the problem is shown in Fig. 2. A parabolic velocity profile is applied on the inlet while the zero pressure condition is applied on the outlet. Non-slip conditions are enforced on the wall and cylinder boundaries. The dynamic viscosity is  $\mu = 5 \times 10^{-3} \text{kg}/(\text{m} \cdot \text{s})$  and the density is  $\rho = 1 \text{kg}/\text{m}^3$ . The gravity is ignored in both cases. The proposed PINN is implemented on the TensorFlow [13], a well documented deep learning platform.

#### 3.1. Steady flow

For the steady case, we ignore the partial derivatives with respect to time. The normal velocity profile is defined as follows

$$u(0, y) = 4U_{\max}(H - y)y/H^2 \quad (5)$$

with  $U_{\max}$  equal to 1.0 m. A small Reynolds number is considered on the inlet to ensure the flow is dominated by laminar flow. The DNN has 7 layers, each with 40 nodes. 50000 collocation points are generated via Latin hypercube sampling (LHS) within the computation domain for the loss function evaluation. It is noted that the distribution of the collocation points is refined near the cylinder to better capture the details of the flow. The Limited-memory BFGS (L-BFGS) optimizer [14] is employed to train the composite DNN due to its good convergence speed demonstrated in the tests.

The predicted velocity and pressure fields by the proposed PINN are shown in Fig. 3(a). To examine the accuracy of the present results, we also compute the reference solutions by the open-source FEniCS solver (finite element-based) [15] and the ANSYS Fluent 18.1 package (finite volume-based) [16] for comparison (see Fig. 3(b)-(c)). It can be observed that the steady velocity and pressure fields are well reproduced by the PINN. It is worth mentioning that the pressure distribution on the cylinder surface is of interest for computing the resultant drag and lift forces. To quantitatively examine the pressure predicted by PINN, we compare the pressure distributions obtained by PINN, FEniCS and ANSYS Fluent as shown in Fig. 4. The overall agreement is very good. Nevertheless, the peak pressure predicted by PINN has a discrepancy of about 4% with those obtained by FEniCS and ANSYS Fluent.

#### 3.2. Transient flow

The transient flow with the same computation domain depicted in Fig. 2 is considered in this case. The time duration for the modeling is 0.5 s. Three virtual pressure probes  $P_1(0.15, 0.2)$  m,  $P_2(0.2, 0.25)$  m and  $P_3(0.25, 0.2)$  m are installed on the surface of the cylinder. The flow is initially still while a time-varying parabolic inlet velocity is defined as

$$u(0, y) = 4 \left[ \sin \left( \frac{2\pi t}{T} + \frac{3\pi}{2} \right) + 1 \right] U_{\max}(H - y)y/H^2 \quad (6)$$

where  $U_{\max}$  equals to 0.5 m and the period  $T$  is 1.0 s. The remaining boundary conditions are the same as those in the previous example. The inflow velocity as a function of  $t$  and  $y$  is visualized in Fig. 5. The width and layer depth of the DNN are selected to be 50 and 7, respectively. 120000 collocation points are used to train the PINN using the L-BFGS optimizer.

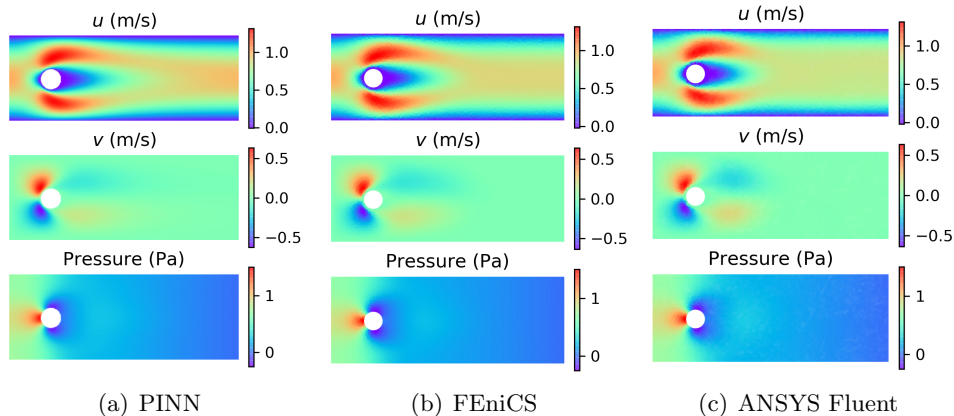


Figure 3: Velocity and pressure fields of the steady flow passing a circular cylinder.

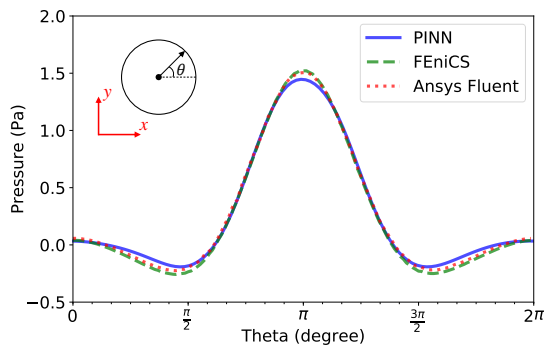


Figure 4: Distributions of pressure on cylinder surface.

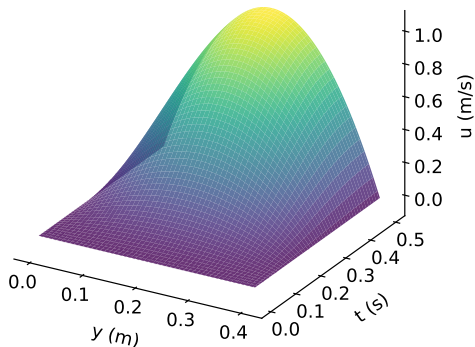


Figure 5: Transient normal velocity profile.

Three snapshots of the predicted flow fields are presented in Fig. 3.2 which shows the evolution of the flow as the inlet velocity increases over time. The reference flows obtained by ANSYS Fluent are not shown here since the PINN-predicted result matches very well with them. The pressure time histories on three probes obtained by PINN are compared with those by ANSYS Fluent as depicted in Fig. 7. It is seen that the proposed PINN approach can well

predict the pressure time histories in a transient flow.

#### 4. Conclusions

We propose a mixed-variable PINN scheme for modeling fluid flows, with particular applications to incompressible laminar flows. The salient features of the proposed scheme include (1) employing the general continuum equations together with the material constitutive law rather than the derived Navier-Stokes equations, and (2) using stream function to ensure the divergence free condition of the flow in a mixed-variable setting. In both the steady and transient flow cases, the result produced by the PINN shows a good agreement with the reference numerical solutions. However, it is notable that the applications in this paper are limited to the laminar flows at low Reynolds numbers, even though the proposed approach is in theory applicable to turbulent flows at large Reynolds numbers. However, it requires discretizing the computation domain with much finer collocation points which will lead to computer memory issues and drastically increase the computational cost. Our future work aims to address this challenge by developing a “divide-and-concur” training scheme in the context of transfer learning.

#### References

- [1] S. Lee, N. Baker, Basic research needs for scientific machine learning: Core technologies for artificial intelligence, Tech. rep., USDOE Office of Science (SC)(United States) (2018).
- [2] R. Zhang, Z. Chen, S. Chen, J. Zheng, O. Bykztrk, H. Sun, Deep long short-term memory networks for nonlinear structural seismic response prediction, Computers & Structures 220 (2019) 55 – 68.

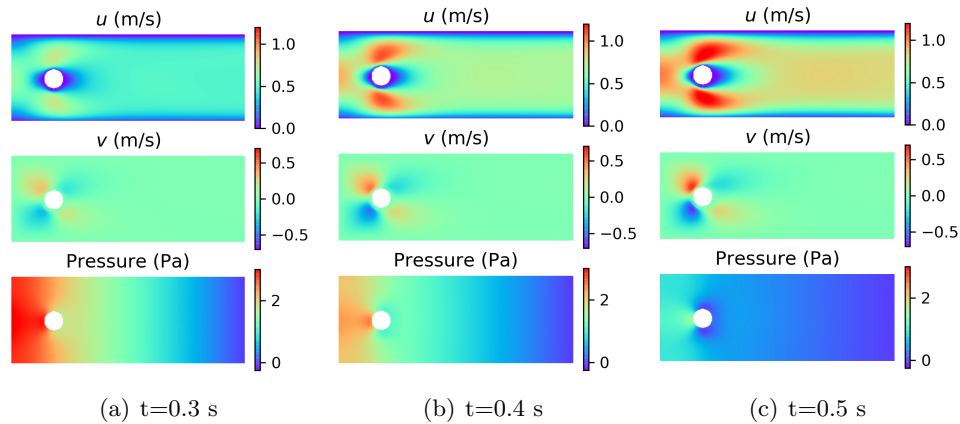


Figure 6: Snapshots of the PINN-predicted transient flow fields passing a circular cylinder

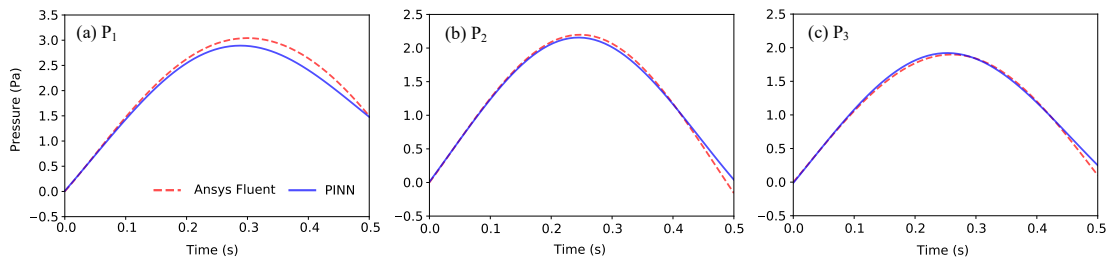


Figure 7: Pressure time histories on  $P_1$ ,  $P_2$  and  $P_3$  probes.

- [3] C. Yang, X. Yang, X. Xiao, Data-driven projection method in fluid simulation, *Computer Animation and Virtual Worlds* 27 (3-4) (2016) 415–424.
- [4] J. Tompson, K. Schlachter, P. Sprechmann, K. Perlin, Accelerating eulerian fluid simulation with convolutional networks, in: *Proceedings of the 34th International Conference on Machine Learning-Volume 70*, JMLR. org, 2017, pp. 3424–3433.
- [5] M. Raissi, P. Perdikaris, G. E. Karniadakis, Physics-informed neural networks: A deep learning framework for solving forward and inverse problems involving nonlinear partial differential equations, *Journal of Computational Physics* 378 (2019) 686–707.
- [6] M. Raissi, Z. Wang, M. S. Triantafyllou, G. E. Karniadakis, Deep learning of vortex-induced vibrations, *Journal of Fluid Mechanics* 861 (2019) 119–137.
- [7] N. Geneva, N. Zabararas, Quantifying model form uncertainty in reynolds-averaged turbulence models with bayesian deep neural networks, *Journal of Computational Physics* 383 (2019) 125–147.
- [8] I. E. Lagaris, A. Likas, D. I. Fotiadis, Artificial neural networks for solving ordinary and partial differential equations, *IEEE transactions on neural networks* 9 (5) (1998) 987–1000.
- [9] I. E. Lagaris, A. C. Likas, D. G. Papageorgiou, Neural-network methods for boundary value problems with irregular boundaries, *IEEE Transactions on Neural Networks* 11 (5) (2000) 1041–1049.
- [10] G. Kissas, Y. Yang, E. Hwuang, W. R. Witschey, J. A. Detre, P. Perdikaris, Machine learning in cardiovascular flows modeling: Predicting arterial blood pressure from non-invasive 4d flow mri data using physics-informed neural networks, *Computer Methods in Applied Mechanics and Engineering* 358 (2020) 112623.
- [11] L. Sun, H. Gao, S. Pan, J.-X. Wang, Surrogate modeling for fluid flows based on physics-constrained deep learning without simulation data, *Computer Methods in Applied Mechanics and Engineering* (2019) 112732.
- [12] Y. Zhu, N. Zabararas, P.-S. Koutsourelakis, P. Perdikaris, Physics-constrained deep learning for high-dimensional surrogate modeling and uncertainty quantification without labeled data, *Journal of Computational Physics* 394 (2019) 56–81.
- [13] M. Abadi, P. Barham, J. Chen, Z. Chen, A. Davis, J. Dean, M. Devin, S. Ghemawat, G. Irving, M. Isard, et al., Tensorflow: A system for large-scale machine learning, in: *12th USENIX Symposium on Operating Systems Design and Implementation*, 2016, pp. 265–283.
- [14] R. Byrd, P. Lu, J. Nocedal, C. Zhu, A limited memory algorithm for bound constrained optimization, *SIAM Journal on Scientific Computing* 16 (5) (1995) 1190–1208. doi:10.1137/0916069.
- [15] A. Logg, K.-A. Mardal, G. Wells, Automated solution of differential equations by the finite element method: The FEniCS book, Vol. 84, Springer Science & Business Media, 2012.
- [16] ANSYS Fluent 18.1, ANSYS FLUENT Theory Guide, ANSYS Inc., PA, USA, 2018.